Heliyon 9 (2023) e14349

Contents lists available at ScienceDirect

Heliyon

journal homepage: www.cell.com/heliyon

Research article

MSCs-laden silk Fibroin/GelMA hydrogels with incorporation of platelet-rich plasma for chondrogenic construct

Dong Chen [a,1], Pengbo Chang [b,1], Peng Ding [c,1], Shuang Liu [d,1], Qi Rao [e], Oseweuba Valentine Okoro [f], Lingling Wang [g,****], Lihong Fan [d,***], Amin Shavandi [f,**], Lei Nie [c,f,*]

[a] Department of Orthopedics, Affiliated Hospital of Jianghan University, Wuhan 430015, China
[b] Zhengzhou Technical College, Zhengzhou 450121, China
[c] College of Life Sciences, Xinyang Normal University (XYNU), Xinyang 464000, China
[d] School of Resources and Environmental Engineering, Wuhan University of Technology, Wuhan 430070, China
[e] Department of Orthopedics, Wuhan Hanyang Hospital, Wuhan University of Science and Technology, Wuhan 430050, China
[f] Université libre de Bruxelles (ULB), École polytechnique de Bruxelles, 3BIO-BioMatter, Avenue F.D. Roosevelt, 50 - CP 165/61, 1050 Brussels, Belgium
[g] Analysis & Testing Center, Xinyang Normal University, Xinyang 464000, China

ARTICLE INFO

Keywords:
Silk fibroin
Gelatin methacrylate
Hydrogel
Cartilage
Platelet-rich plasma

ABSTRACT

Repair of osteochondral defects and regeneration of cartilage is a major challenge. In this work, the mesenchymal stem cells (MSCs)-laden hydrogel was designed using silk fibroin (SF) and gelatin methacrylate (GelMA), to encapsulate platelet-rich plasma (PRP). Initially, GelMA was synthesized, and SF was prepared using silkworm cocoon, then MSCs-laden SF/GelMA (SG) hydrogel was fabricated. The physicochemical properties of the hydrogels were evaluated using Fourier-transform infrared spectroscopy, scanning electron microscope, and rheometry. After hydrogel preparation, the viability of MSCs in the hydrogels was investigated via CCK-8 analysis and fluorescent images. The MSCs-laden SG hydrogel containing PRP was subsequently injected into the cartilage defect area in Sprague Dawley rats. Hematoxylin and eosin (H&E), Masson staining, and Mankin scores evaluation confirmed the new cartilage formation in 8 weeks. The results presented in the study, therefore, showed that the prepared MSCs-laden SG hydrogel loaded with PRP has the potential for cartilage reconstruction, which is crucial to the treatment of knee osteoarthritis.

* Corresponding authors. College of Life Sciences, Xinyang Normal University (XYNU), Xinyang 464000, China.
** Corresponding author. Université libre de Bruxelles (ULB), École polytechnique de Bruxelles, 3BIO-BioMatter, Avenue F.D. Roosevelt, 50-CP 165/61, 1050 Brussels, Belgium.
*** Corresponding authors. School of Resources and Environmental Engineering, Wuhan University of Technology, 122 Luoshi Road, Wuhan, Hubei, 430070, China.
**** Corresponding author.
E-mail addresses: LingLingWang@xynu.edu.cn (L. Wang), lihongfan2000@hotmail.com (L. Fan), amin.shavandi@ulb.be (A. Shavandi), nieleifu@yahoo.com, nielei@xynu.edu.cn (L. Nie).
[1] There authors contributed equally to this work and should be considered co-first authors.

https://doi.org/10.1016/j.heliyon.2023.e14349
Received 22 November 2022; Received in revised form 24 February 2023; Accepted 2 March 2023
Available online 9 March 2023

1. Introduction

Knee osteoarthritis (KOA) is a common degenerative joint disease that is usually caused by ageing, obesity, trauma, congenital abnormality and deformity [1]. The articular cartilage is most commonly involved in KOA, which is manifested as hyperplasia of articular borders and subchondral bone and degeneration of articular cartilage [2]. KOA has become a significant cause of disability and causes severe economic burdens to patients and the healthcare system worldwide [3]. KOA could be treated using physical modalities and exercise, complementary and alternative medicine, pharmacologic treatment, intra-articular injections, and surgery [4]. The physical modalities for KOA patients include physical therapy interventions, exercise, weight loss, and braces or heel wedges and pharmacological with the effectiveness of using different treatment interventions considered variable [4–7]. The pharmacologic treatments could also be categorized as topical, oral, and intra-articular [8]. Intra-articular injections may relieve the short-term symptom of patients with a low risk of adverse effects [9,10]. Usually, the surgery includes arthroscopic surgery and total knee replacement, and total knee arthroplasty (TKA) is considered a last resort [11]. The targets of most treatments on KOA are the predominant symptom of pain and cartilage damage, with non-surgical treatments focused on relieving the early-stage symptoms of KOA. Mainly, the surgical approaches are still limited by the risk of the formation of fibrocartilage, which may hinder the recovery of the functional properties of the native cartilage tissue [12,13].

The application of regenerative engineering strategies, such as the convergence of stem cells, scaffold, and growth factors, will enable the development of translational therapies for KOA treatment [14–16]. In this regard, a wide variety of biomaterials have been used to deliver cells [17] and growth factors (i.e. using hydrogel) to promote the regeneration of cartilage tissues [18]. Hydrogels are three-dimensional (3D) polymeric networks with a high amount of water, which mimic the native extracellular matrix (ECM) [19,20]. Such as, injectable hydrogels could quickly and easily fill defects of any size and shape in a minimally invasive manner. Also, the cells and bioactive molecules could be delivered to the target site [21–24]. The protein-based polymers could facilitate the selective adsorption of bioactive molecules that could more effectively influence cell fate for enhanced cartilage repair [25]. Additionally, the properties of proteins, such as silk fibroin (SF), have been reported to be tunable since SF contains several oxidizable tyrosine groups, for the production of covalent dityrosine crosslinks. These cross-links present a pathway to enable the regulation of SF properties for enhanced cartilage regeneration [26–28]. Another protein-based polymer, gelatin methacrylate (GelMA), has also been reported to be capable of promoting cartilage repair due to its excellent biocompatibility, biodegradability and bioactivity properties [29,30]. Hou et al. [31], fabricated SF/GelMA scaffold laden with melatonin (MT) to promote cartilage regeneration in a full-thickness cartilage defect model. Xiao et al. [32], also designed SF/GelMA hydrogel via sonication and photocrosslinking for encapsulating cells or growth factors. In addition, Hong et al. [33], 3D printed SF/glycidyl-methacrylate using digital lighting processing (DLP) printer for chondrocyte encapsulation, and in vivo experiments demonstrated the new cartilage-like tissue and epithelium found surrounding transplanted hydrogel. Therefore, SF and GelMA were employed in the fabrication of hydrogels for improving chondrocyte viability and chondrogenic differentiation for the regeneration of cartilage defects.

In addition, it is recognised that mesenchymal stem cells (MSCs) are recruited during the chondrogenesis process to proliferate and differentiate into a chondrogenic phenotype. Indeed, MSCs have attracted much attention for KOA treatment, and the MSCs composited with HA are already developed in the clinical trial stage as phase I in Taipei Medical University Hospital (Gov Identifier: NCT04893174). Zheng et al. [34], fabricated MSCs seeded SF/GelMA hydrogel with an interpenetrating network (IPN) for articular cartilage repair. The gene expressions of *Col-2*, *Acan*, and *Sox-9* were significantly higher in MSCs seeded SF/GelMA hydrogel in

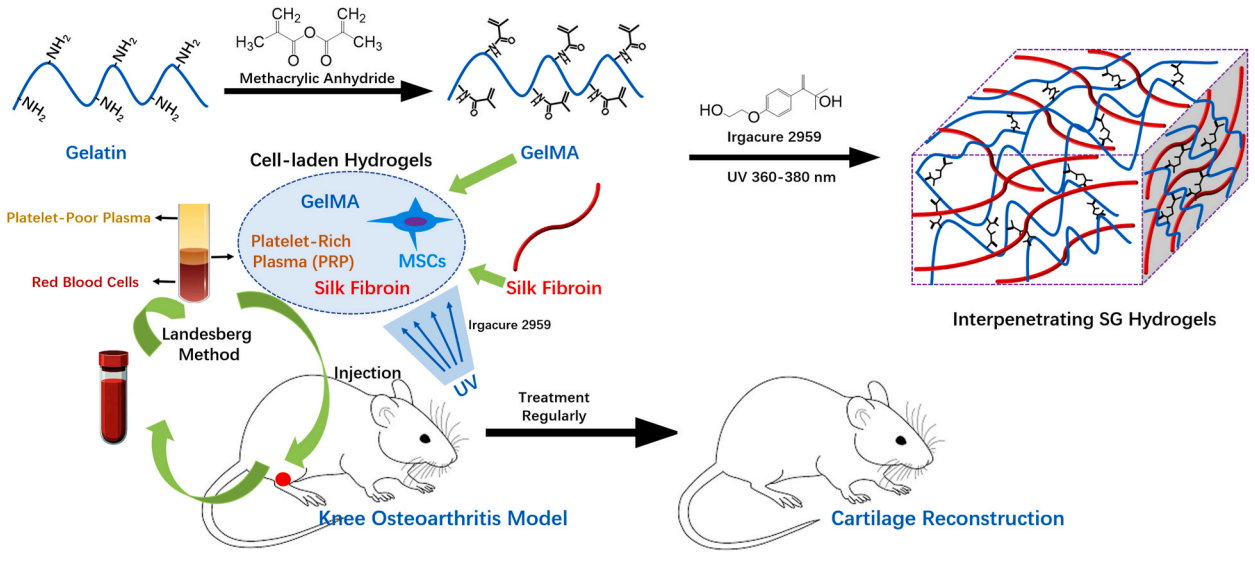

Scheme 1. A schematic illustration of the preparation of MSCs-laden gelatin methacrylate/silk fibroin (GelMA/SF, SG) hydrogel with the incorporation of PRP for treating KOA to reconstruct cartilage.

comparison with pure GelMA hydrogel. Many animal models and some clinical cases have proved the chondrogenic potential of MSCs in bone marrow for the treatment of KOA [35]. In addition, the use of MSCs-laden hydrogels for KOA treatment could circumvent the limitations of autologous chondrocyte implantation (ACI), which could achieve the equivalent clinical results as the first-generation ACI in the last 10 years without the increased risk of tumour formation [36].

It has also been reported that growth factors and hormones such as transforming growth factors (TGFs), insulin-like growth factors (IGFs), bone morphogenetic proteins (BMPs), and dexamethasone can promote the chondrogenic or osteogenic differentiation of MSCs [37]. Thus, a hydrogel combining both cells and growth factors could be used for KOA treatment as the next generation of engineered osteochondral/cartilage constructs [38]. Notably, platelet-rich plasma (PRP) injection has received increasing interest in KOA treatment in recent years. PRP is an autologous blood product that contains an increased concentration of platelets than whole blood, and the plasma contains cytokines, thrombin, and other growth factors, the degranulation of the platelets releases growth factors [39, 40]. The use of PRP as a treatment for KOA is straightforward and limits adverse drug interactions due to PRP from the patient's own proteins [41].

In this study, the MSCs-laden hydrogel (SG) based on SF and GelMA with IPN structure was fabricated first, and PRP was prepared from SD-rats. Then, the MSCs-laden SG hydrogel with the incorporation of PRP was fabricated. The physicochemical properties of SG hydrogels were evaluated. The viability of MSCs in SG hydrogel was evaluated using CCK-8 analysis and fluorescent images. Next, the cartilage reconstruction ability of MSCs-laden SG hydrogel with the incorporation of PRP was investigated by injecting into SD rats, the cartilage formation after 8 weeks was investigated using Hematoxylin and eosin (H&E) and Masson staining, and Mankin scores (Scheme 1).

2. Materials and methods

2.1. Chemicals

The cocoon shell of *Bombyx Mori* silkworm was purchased from Chihe town, Shaanxi, China. Gelatin type A (300 bloom from porcine skin) was purchased from Merck Co., Ltd. Sodium phosphate dibasic dodecahydrate ($Na_2HPO_4{\cdot}12H_2O$) and sodium hydroxide (NaOH) were purchased from Sinopharm Co., Ltd. Calcium chloride anhydrous ($CaCl_2$) and sodium carbonate (Na_2CO_3) were obtained from Macklin Co., Ltd. Methacrylic anhydride (MA) was purchased from Sigma-Aldrich Co., Ltd. Irgacure 2959 was obtained from BASF Co., Ltd. All chemicals and solvents purchased were used as received without further purification.

2.2. Synthesis of gelatin methacrylate (GelMA)

The GelMA was synthesized according to the method described in the literature [42,43]. Briefly, type A gelatin was mixed with phosphate buffered saline (PBS) solution at 60 °C and stirred until fully dissolved (10 w/v%). The MA was then added to the gelatin solution in a dropwise manner and stirred for 4 h at 50 °C. After then, the reaction was stopped by diluting 5 × using warm PBS (50 °C) with the resulting mixture dialyzed for one week at 40 °C against distilled water while using a cutoff dialysis tubing (SMWCO 12–14 kDa) to remove salts and unreacted MA. The solution was finally lyophilized for 72 h to generate white porous foam and stored at −20 °C until further use.

2.3. Extraction of silk fibroin (SF)

The SF was extracted from *Bombyx Mori* silk cocoons according to the method described in the literature [44]. Briefly, the silk cocoons were cut and added to a 0.5 M Na_2CO_3 solution and boiled for 30 min. Then, the extracted SF was recovered and cleaned by washing with deionized water 5–6 times, and dried in an oven at 50 °C for 24 h. After this, the dried SF was cut into pieces again and dissolved in $CaCl_2$ solution (10 w/w%) to obtain SF solution, and the above SF solution was added to ethanol and water mixed solution (1:4 v/v) at 70 °C and stirred for 5 h. Subsequently, the sample was dialyzed for 4 days against distilled water. Finally, the sample was separated by centrifugation (12,000 rpm, 10 min for each time) 3 times and freeze-dried to obtain SF.

2.4. Preparation of SF/GelMA (SG) hydrogels

First, SF was dissolved in phosphate buffer to obtain SF solution (5 w/v%). The SF solution, GelMA, and Irgacure 2959 were then added to a centrifuge tube, and a 3 mL phosphate buffer was added and oscillated until evenly mixed, and the total concentration of polymers was maintained at 8 w/v%. The solution was exposed using UV-light irradiation for ~30 s to obtain SG hydrogel. In this

Table 1
The designation of the silk fibroin/gelatin methacrylate (SG) hydrogels[a].

SG Hydrogels	SG-1	SG-2	SG-3
Silk fibroin [b]	2.1 mL	2.1 mL	2.1 mL
Gelatin methacrylate	240 mg	270 mg	300 mg

[a] 15 mg of Irgacure 2959 was used for all SG hydrogels.
[b] The silk fibroin is dissolved in phosphate buffer, and the concentration is 5 w/v%.

study, 3 types of SG hydrogels using different ratios of SF/GelMA were prepared (Table 1).

2.5. Characterization

2.5.1. Scanning electron microscopy (SEM) analysis

The morphology of the cross-section of SG hydrogels was characterized using SEM. The liquid nitrogen was used to freeze the lyophilized SG hydrogels rapidly, and the samples were subsequently cut off to investigate their cross-section. The obtained samples were sprayed using platinum for 40 s, and the morphologies of the samples were subsequently observed using a cold field emission scanning electron microscopy (SEM, Hitachi, S-4800).

2.5.2. Fourier-transform infrared spectroscopy (FT-IR) analysis

The presence of specific chemical groups in SG hydrogels was investigated using FT-IR (ThermoFisher, Nicolelis5). The FT-IR spectra of freeze-dried SG hydrogels were obtained using the attenuating total reflection (ATR) technique between 4000 and 500 cm^{-1}.

2.5.3. Rheology analysis

A rheometer (TA, DHR, USA) was used to evaluate the rheological property of the prepared SG hydrogels. Briefly, a 0.5 mL aliquot of SC hydrogels was loaded to the temperature-controlled Peltier bottom plate (37 °C) using a 20 mm stainless steel upper cone. Low-viscosity oil was placed around the outside edge of the cone to prevent water evaporation. The storage modulus (G′), loss modulus (G″), and viscosity were recorded in terms of angular frequency (0.1–140 rad/s).

2.5.4. Degradation rate

The degradation rate of SG hydrogels was evaluated by soaking in PBS [45]. The dried SG hydrogel was weighed as W_0 and then soaked in PBS (solid/liquid ratio: 50 mg/mL), and kept at 37 °C for 8 weeks. The samples were rinsed using distilled water and weighed as W_t at different predefined time intervals. The degradation rate was calculated as follows (equation (1)) :

$$Remaining\ weight\ (\%) = \frac{W_t}{W_0} \times 100\ \% \tag{1}$$

2.6. Cell culture

Due to the potential differentiation into cartilage cells (chondrocytes), bone marrow-derived mesenchymal stem cells (MSCs, Normal, Human, ATCC®PCS-500-012™) were used in this work. The MSCs culture was operated according to ATCC instruction, MSCs were grown in Dulbecco's modified Eagle's medium (DMEM) (Sigma-Aldrich) with 10% fetal bovine serum, and 1% of a 100 mg/mL mixture of penicillin and streptomycin under a humidified atmosphere (5 v/v% CO_2 and 95 v/v% air) at 37 °C. The cell medium was replaced every 2 days, and the cells at passage 5 for the preparation of MSCs-laden SG hydrogels.

2.7. Preparation of MSCs-laden SG hydrogels

The MSCs-laden SG hydrogel was prepared according to our previous work [46]. First, the MSCs were digested and dispersed in a DMEM medium containing 10% fetal bovine serum, and 1% of a 100 mg/mL mixture of penicillin and streptomycin. The SF solution, GelMA, and Irgacure 2959 were then added in an MSCs dispersed medium (1×10^4 cells/mL), and the mixed suspension was gently oscillated until fully mixed. The obtained cell suspension was gelled using UV-light irradiation for 30 s, and the prepared MSCs-laden SG hydrogel was subsequently placed in an incubator of 37 °C. The cell growth status was investigated using optical microscopy and confocal laser scanning microscope (CLSM, Leica TCS SP5 II, Germany) using 4′6-diamidino-2-phenylindole (DAPI) and phalloidin-FITC staining. And the cell viability of MSCs in SG hydrogels was quantitatively evaluated using cell counting kit-8 (CCK-8), and the optical density (O.D) at 450 nm each day was recorded using a microplate reader (Tecan GENios, Tecan Austria GmbH, Salzburg, Austria) [47], and the experiment was conducted in triplicate.

2.8. Preparation of platelet-rich plasma (PRP)

PRP was obtained from Sprague–Dawley (SD) rats using the Landesberg method [48,49]. The SD rats were kept in the Institute of Experimental Animals of Huazhong University of Science and Technology in accordance with the institutional guidelines for the care and use of laboratory animals. The whole blood (WB) was obtained by venipuncture in an acid citrate dextrose (ACD) tube from SD rats (8-week-old, 200–250 g, SPF). WB was centrifuged 2 times to obtain PRP. First, WB was centrifuged at 200×*g* for 10 min, and the upper layer with the buffy coat was transferred to an empty sterile tube. Then, the tube was centrifuged at 200×*g* for 10 min again, and after then, the solution was separated into two layers, the upper layer was platelet-poor plasma (PPP), and the lower layer was platelet concentrate (PC). PPP was removed, and PC was suspended in a minimum quantity of plasma by gently shaking the tube to obtain PRP. All animals were treated in accordance with the "Principles of Laboratory Animal Care" (NIH publication #85-23, revised 1985).

2.9. Knee osteoarthritis (KOA) animal model

The animal experiments were approved by the Animal Ethical Committee of Wuhan Hanyang Hospital (Wuhan University of Science and Technology). The KOA animal model was replicated using a modified Hulth's modelling method [1,50]. First, the SD rats (8-week-old, 200–250 g, SPF) were anaesthetized using 1% of sodium pentobarbital (40 mg/kg). Then, an incision was made in the right knee, and cartilage, meniscus and other structures were examined to all be in good condition prior to the next operation. The cruciate ligament and medial collateral ligament were cut off, and the medial meniscus was separated and removed. The articular cavity and incision were then flushed using physiological saline and sutured with 0.5 mL of glutaraldehyde (4%) injected into the articular cavity. The wounds were then closed using routine techniques. After the operation, levofloxacin hydrochloride (8 mg/kg, every 12 h) and sodium chloride (100 mL) were intravenously injected to prevent infection within 3 days, and tramadol hydrochloride (8 mg/kg) was intramuscularly injected to relieve pain.

2.10. Animal experiments

In this work, the four groups (6 rats per group) were designed based on the replicated KOA animal model. Group A: the blank control group without intervention; Group B: SG hydrogel was injected into the articular cavity; Group C; SG hydrogel with PRP was injected into the articular cavity; Group D: MSCs-laden SG hydrogel with PRP was injected into the articular cavity. For Group B, C, and D, the injection volume was 0.1 mL, and the injection frequency was 1 time/1 week. The SG hydrogel with the highest storage modulus and best cytocompatibility was used for the animal experiments.

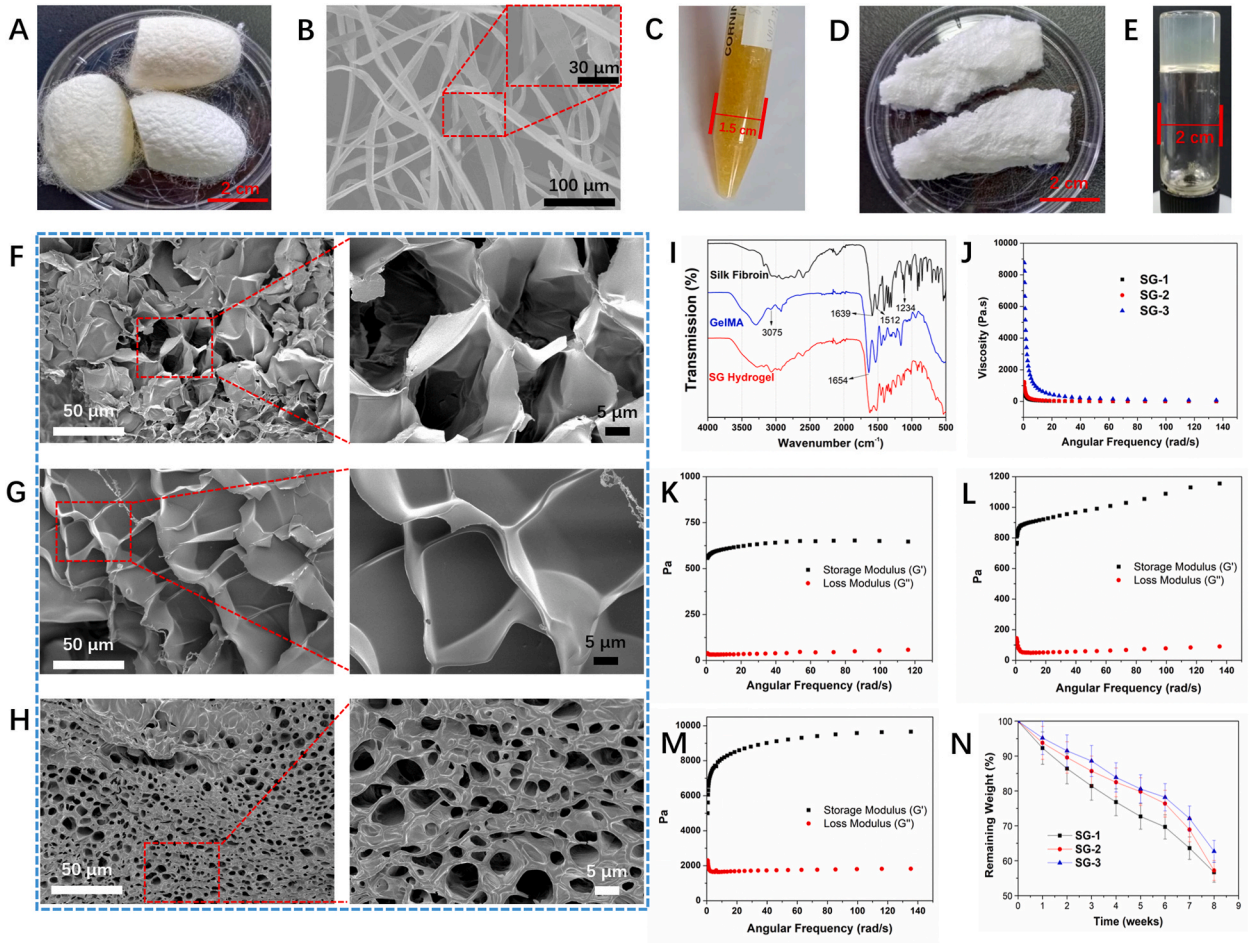

Fig. 1. (**A**) The morphology of silkworm cocoon for preparation of silk fibroin (SF); (**B**) SEM images of the synthesized SF, the image inserted in the top-right corner was enlarged at a higher magnification; (**C**) The photo of the obtained SF; (**D**) The photo of the synthesized GelMA polymer; (**E**) The formation of SG hydrogel could be confirmed using a tube inversion method; SEM images of SG hydrogels at a dry state, (**F**) SG-1, (**G**) SG-2, (**H**) SG-3, the SEM images in the right row were enlarged from the left row at higher magnifications; (**I**) The FT-IR spectra of SF, GelMA, and SG-1 hydrogel; (**J**) The change of viscosity of SG hydrogels in term of frequency; The change of storage modulus (G′) and loss modulus (G″) of (**K**) SG-1, (**L**) SG-2, and (**M**) SG-3 hydrogels in term of frequency; (N) The degradation curves of SG hydrogels in PBS for 8 weeks.

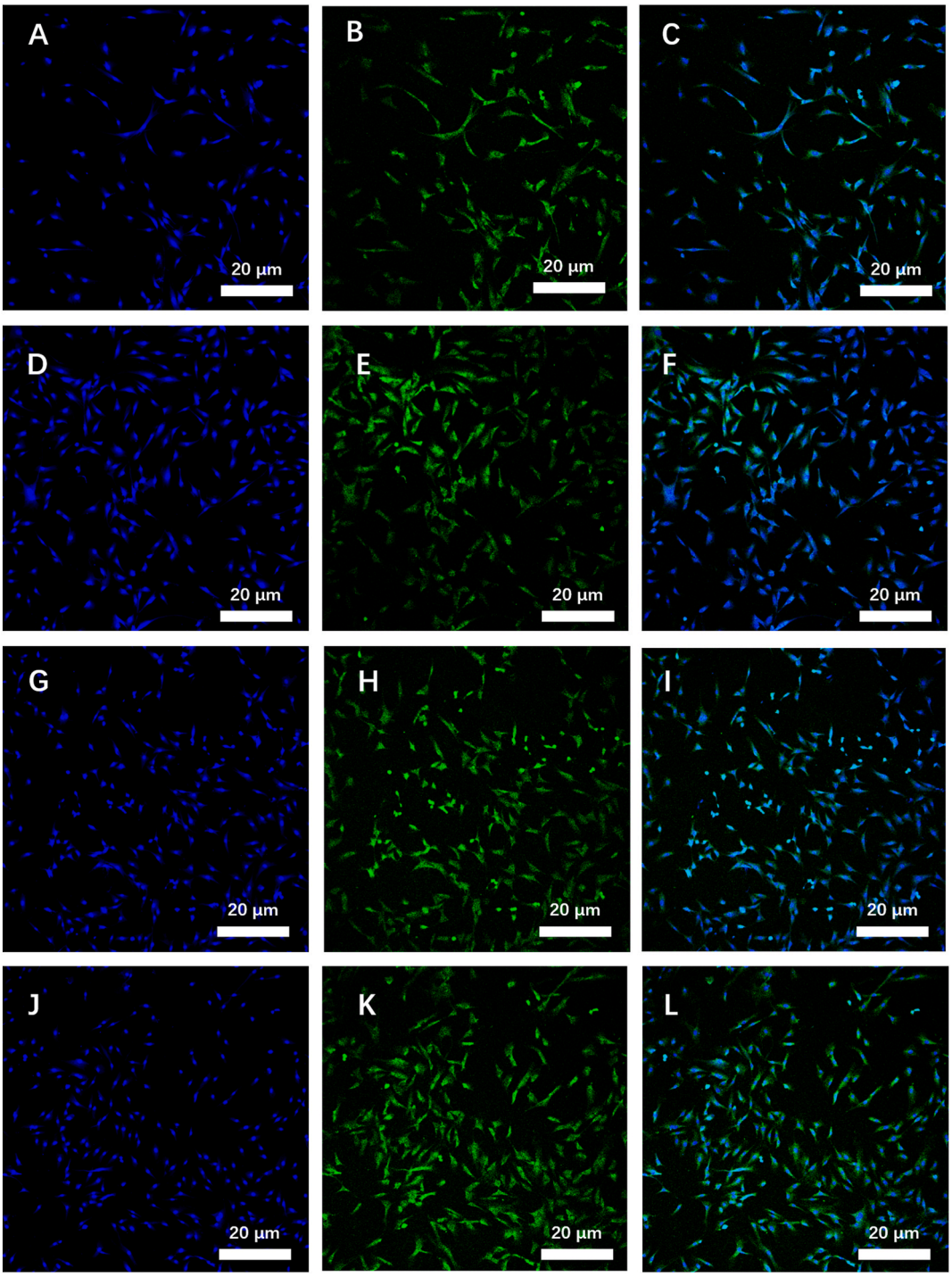

Fig. 2. The MSCs proliferation after loaded in SG hydrogels and cultured for 72 h, cells cultured without hydrogel as a control group. Laser scanning confocal microscope (LSCM) images of MSCs loaded in SG-1 (**A**, **B**, and **C**), SG-2 (D, E, and F), and SG-3 (**G**, **H**, and **I**) hydrogels, and without hydrogels (**J**, **K**, and **L**) cultured for 72 h, images (**A**, **D**, **G**, and **J**) displayed that cell nucleus stained using DAPI as shown in blue color, images (**B**, **E**, **H**, and **K**) displayed that cytoskeleton stained using Phalloidin-FITC as shown in green color, and image (**C**, **F**, **I**, and **L**) was merged from DAPI, and Phalloidin-FITC stained images, respectively. (For interpretation of the references to color in this figure legend, the reader is referred to the Web version of this article.)

2.11. Histological examination

The SD rats were euthanised after 8 weeks post-surgery. The biopsies of the knee-joint were obtained. The biopsies were fixed in 10% neutral formalin for 1 day, decalcified in 10% EDTA for 1 week at 37 °C, dehydrated in ascending grades of ethanol, and then embedded in paraffin. The cartilage reconstruction was investigated using hematoxylin-eosin (HE) and Masson stains for optical microscopy observation. In addition, the reconstructed cartilage was scored using the Mankin Scoring system [51,52]. Based on the structure (0–6), cellular abnormalities (0–3), stromal staining (0–4), and integrity (0–1), the Mankin scores of each group were obtained. Furthermore, 0 was used to indicate the normal cartilage, and 14 was used to indicate the most severely defective cartilage. To avoid bias, the observer who gave the Mankin scores under the microscope was unaware of each group in advance.

2.12. Statistical analysis

The data was expressed as means with standard deviation (SD) based on the triplicate experiments. The SPSS software (SPSS Inc, Chicago IL), ANOVA statistical analyses and Tukey's test were applied for the analysis. Statistical significance was defined based on the different p-values: <0.05 for 95%, and <0.01 for 99%.

3. Results and discussion

3.1. SG hydrogels

In this work, SF was extracted from *Bombyx Mori* silk cocoons (Fig. 1A). SF needs to be purified from silk cocoons by removing the silk sericin via degumming [53]. SEM images observed that the degummed SF displayed a smooth surface without silk sericin remains, and no damaged structure was observed on the surface of SF (Fig. 1B). The light-yellow liquid SF was obtained without odour (Fig. 1C). The cross-sectional morphologies of the freeze-dried SG hydrogels were investigated using SEM images, as shown in Fig. 1F–H. The SG hydrogels were determined to have a connected structure. Apparently, the pore size of SG hydrogels was gradually decreased with increasing the GelMA ratio in hydrogels, mainly due to the increase of cross-linking density. The cross-linking of GelMA in SG hydrogels further contributed to the cross-linking density of SG hydrogels, and the morphology of SG hydrogels was greatly influenced by the cross-linking density [54,55]. The successful preparation of SF was confirmed using FT-IR, as shown in Fig. 1I. Fig. 1I shows the peaks at 1662 cm^{-1}, 1529 cm^{-1}, 1244 cm^{-1} and 678 cm^{-1}, which correspond to the amide I band, amide II, amide III, and amide V, respectively. On the other hand, GelMA was synthesized using gelatin and methacrylic anhydride, and the white porous GelMA was obtained (Fig. 1D) [56]. The FT-IR spectrum of GelMA (Fig. 1I), shows the peaks at 3075 cm^{-1} and 1654 cm^{-1}, which are due to signals from N–H stretching and amide I, respectively. This result indicates that gelatin was chemically modified to form GelMA. Furthermore, the shift of peak at 3075 cm^{-1} for the spectrum of SG hydrogel confirms the interaction between SF and GelMA in SG hydrogel. The formation of SG hydrogels was assessed using the tube inversion method (Fig. 1E) [15,21,57]. Compared to the FT-IR spectra of SF and GelMA, new vibration peaks were not observed for SG hydrogels, confirming that there was no chemical interaction between SF and GelMA (Fig. 1I). Furthermore, the storage modulus (G′) and loss modulus (G″) of SG hydrogels at 37 °C were investigated (Fig. 1J-M). Both G′ and G″ of SG hydrogels increased during the solution-to-hydrogel formation process as the GelMA content in hydrogels increased. This observation was due to the increase in the photo-cross-linked degree as more interpenetrating networks of GelMA were introduced. After the formation of hydrogels, the viscosity of SG hydrogels decreased as the angular frequency increased, highlighting the shear-thinning property of SG hydrogels. *In vitro* biodegradation property of SG hydrogels was investigated by soaking in SBF, and

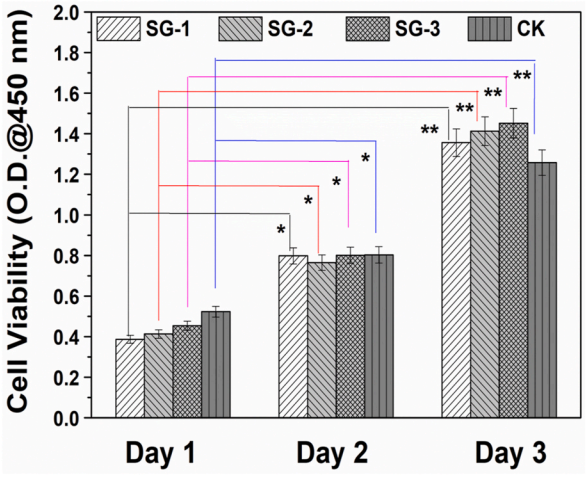

Fig. 3. Cell viability of MSCs after loaded in SG hydrogels and cultured for different days. *$p < 0.05$, and **$p < 0.01$.

the remaining weight was calculated at predetermined days, as shown in Fig. 1N. The weight loss of SG hydrogels increased over-soaking days, and the weight loss decreased with increasing the ratio of GelMA in SG hydrogels due to the smaller pore size and higher cross-linking density.

3.2. MSCs-laden SG hydrogel

The SG hydrogels could be formed from solution in 30 s under UV-light irradiation; thus, MSCs could be encapsulated into hydrogels to obtain MSCs-laden SG hydrogels. MSCs would grow and proliferate in SG hydrogels in an incubator of 37 °C. In all SG hydrogels it was observed that the number of MSCs increased, as confirmed using optical microscopy (Fig. S1). Indeed, after 72 h, the morphology of MSCs in SG hydrogels could be investigated using confocal laser scanning microscope (CLSM) images after staining with 4′6-diamidino-2-phenylindole (DAPI) and Phalloidin-FITC (Fig. 2A-L). MSCs displayed a formless morphology in SG-1, SG-2, SG-3 hydrogels, and without loaded in hydrogel, with the nucleus and cytoskeleton of MSCs stained in blue color and green color, respectively. The morphologies of MSCs in SG hydrogels, were clearly observed under bright light, confirming SG hydrogels provided a suitable 3D microenvironment for MSCs growth (i.e. Fig. S1). The MSCs were uniformly dispersed into SG-1 hydrogel, which was clearly observed while merging two CLSM images under a bright light and excitation field (Fig. S1). A simple visual consideration of Fig. 2 shows that higher numbers of MSCs are present in the SG-3 and SG-2 hydrogels compared to the SG-1 hydrogels although the MSCs number could not be quantitatively analyzed using only fluorescent images. The CCK-8, therefore, needs to be used to evaluate the growth and proliferation of MSCs in SG hydrogels.

MSCs viabilities in SG hydrogels were therefore quantitatively evaluated using cell counting kit-8 (CCK-8), and the optical density (O.D) at 450 nm subsequently recorded on different days, as shown in Fig. 3. Fig. 3 also shows that the differences in cell viabilities of the MSCs in day 2 and day 3 relative to the cell viability of MSCs in day 1 for SG-1, -2 and -3 are statistically significant. It is also seen that the viability of MSCs encapsulated in the hydrogels increased from day 1 to day 3, indicating a good cytocompatibility of all SG hydrogel samples. On day 1, O.D values for all SG hydrogels were lower than that of the control group. However, O.D values for all samples were higher than that of the control group on day 3, which might be due to the presence of 3D micro-environments in the SG hydrogels that support the proliferation of MSCs. This is because, the hydrogel network mimics the micro-environment of natural tissues, and nutrients and growth factors that can be encapsulated and exchanged in such 3D micro-environment [58].

3.3. Cartilage reconstruction

Next, PRP was prepared from Sprague–Dawley (SD, 8-week-old, 200–250 g, SPF) rats using the Landesberg method [48,49]. The

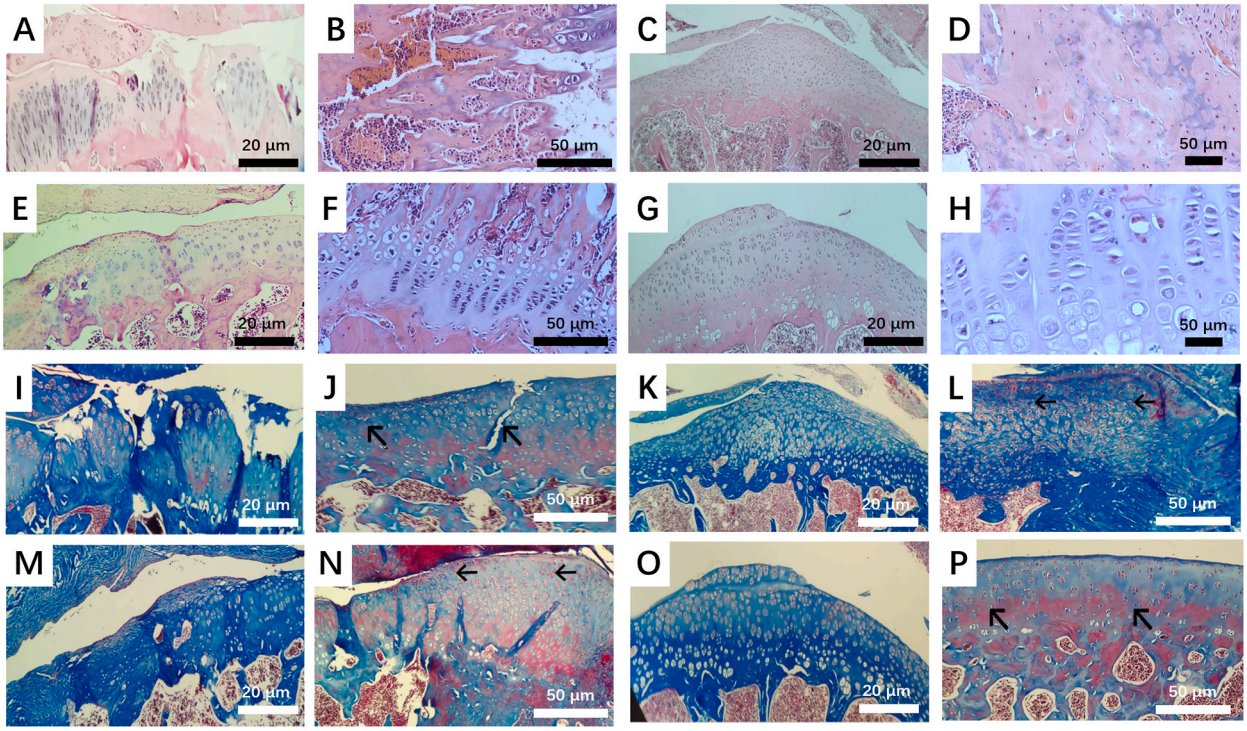

Fig. 4. Optical micrographs of (**A-H**) H&E and (**I–P**) Masson staining slices of tissues after SG hydrogels (**C, D, K,** and **L**), SG hydrogels incorporated with PRP (**E, F, M,** and **N**), and MSCs-laden SG hydrogels incorporated with PRP (**G, H, O,** and **P**) were intra-articular injected into SD rats for 8 weeks, respectively, the SD rats without hydrogels intervention as the control group (**A, B, I,** and **J**).

concentration of PRP in the whole blood (WB) was around 579.84 (±54.12) × 10^6/mL. After centrifuging twice (200×*g*, 10 min for each time), the PRP concentration increased to ~2638.07 (±496.41) × 10^6/mL, which was 5.55 times compared to that of WB. The KOA models were subsequently replicated in SD rats using a modified Hulth's modelling method and the SD rats were treated by injecting SG hydrogel, SG hydrogel with PRP, and MSCs-laden SG hydrogel with PRP into the articular cavity, and without intervention as the blank control group. Crucially, since SG-3 hydrogel displayed the highest storage modulus, and presented the best performance with respect to cell viability of MSCs, the SG-3 hydrogel was selected and employed for animal experiments. After 8 weeks, cartilage recovery was evaluated using hematoxylin-eosin (HE) and Masson stains, and the optical microscopy images shown in Fig. 4. The bone MSCs seeded in SG hydrogels displayed higher gene expression levels of *Sox9*, *Acan*, and *Col2a1* than in GelMA hydrogel, proving the chondrogenic differentiation of bone MSCs in SG hydrogels, which was confirmed by the previous work [34]. In the present works, the cartilage reconstruction ability of MSCs laden SG hydrogels with the incorporation of PRP would be in vivo investigated.

For the control group without intervention, the articular cartilage surface was still rough and damaged, the defect area was large, and few chondrocytes were observed, with any chondrocytes present manifested in a disordered arrangement (Fig. 4A, **B**, **I** and **J**). More chondrocytes were discovered for the group with SG hydrogels treatment; however, the defect area still existed, showing that the cartilage could not recover completely when only SG hydrogels were deployed in the absence of MSCs and PRP (Fig. 4C, D, K, and L). For the group treated with SG hydrogels with PRP, the integrity of cartilage was further increased, and more chondrocytes were observed (Fig. 4E, F, M, and **N**). Compared to the above groups, it could be clearly observed that the cartilage was reconstructed entirely using MSCs-laden SG hydrogel with PRP, the surface of the articular cartilage was smooth and flat, and the chondrocytes were evenly arranged regularly, and no joint fissure was observed (Fig. 4G, H, O and **P**).

Lastly, the reconstructed cartilage was evaluated using the Mankin scoring system (Fig. 5), and the scores for the groups treated using SG hydrogel, SG hydrogel with PRP, and MSCs-laden SG hydrogel with PRP were 6.5 ± 0.46, 5.5 ± 0.72, and 3.0 ± 0.91, respectively, which were all lower than that of the control group (12.5 ± 0.50). Compared to the O'Driscoll cartilage repair scoring system [59], Mankin scoring system does not only score cartilage-like tissue characteristics and structural integrity, but also scores cellular abnormalities and stromal staining, and thus is considered as a comprehensive evaluation method in clinical studies [60]. In this work, the immunohistochemical method will be used to evaluate the remodeling process of MSCs-laden SG hydrogel with PRP for further clinical applications. To this regard, Fig. 5 confirmed that the cartilage defect treated with MSCs-laden SG hydrogel with PRP displayed the best cartilage reconstruction than other groups, proving that MSCs-laden SG hydrogel with PRP was effective for KOA treatment.

The results presented thus far show that the combined effects of PRP and MSCs are crucial to promoting the recovery of cartilage defects. This observation is consistent with previous studies in the literature that highlighted the favourable outcome of incorporating PRP in hydrogels to facilitate cartilage defect recovery [61,62]. For instance, in the study by Gao, Gao [63], a hydrogel composed of sodium alginate and PRP was shown to support the proliferation of mesenchymal stem cells derived from the bone marrow and chondrogenesis. Notably, these favourable effects presented a positive correlation with the increase as the PRP concentration. In another study, a construct based on poly(lactic-co-glycolic acid) (PLGA) was laden with MSCs and PRP and shown to be effective in facilitating a simultaneous regeneration of both articular cartilage and subchondral bone within osteochondral defects [64]. Different from Zhang's works [64], the present study employed protein-based biopolymers (SF and gelatin) to culture and deliver MSCs and PRP due to the unique properties of protein-based biopolymers, such as lower immunogenicity, biodegradability, and enhanced biocompatibility [29]. The present study acknowledges that although favourable effects were observed when the MSCs-laden SG hydrogel was employed in promoting the recovery of cartilage defects, more work regarding the mechanical properties of the composite hydrogel must be undertaken. Indeed, optimizing both the mechanical and biological properties of the novel hydrogel will be investigated in future studies.

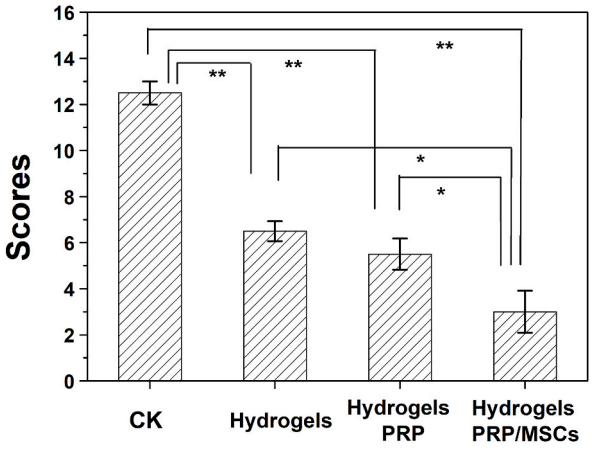

Fig. 5. The obtained scores for SG hydrogel, SG hydrogel with PRP, MSCs-loaded hydrogel with PRP, and control group using Mankin Scoring system. *$p < 0.05$, and **$p < 0.01$.

4. Conclusions

In summary, prepared MSCs-laden SG hydrogel was incorporated PRP which was extracted from the whole blood of SD rats and the resulting PRP containing hydrogel was assessed for its cartilage regeneration properties. In this regard, the physicochemical properties of SG hydrogels were initially investigated using FT-IR, SEM, and rheometer analysis. It was shown that the properties of the SG hydrogels enabled its injection into the articular cavities. Further experimental investigations via CCK-8 and fluorescent image analysis confirmed that MSCs could grow and proliferate in SG hydrogels. The KOA models were then replicated in SD rats, and the MSCs-laden SG hydrogel containing PRP was subsequently injected into the articular cavity. H&E and Masson staining and Mankin scoring system confirmed that the cartilage could be reconstructed in 8 weeks. The obtained results showed that the obtained MSCs-laden SG hydrogel containing PRP has the potential for KOA treatment.

Author contribution statement

Dong Chen, Lei Nie: Conceived and designed the experiments; Performed the experiments; Analyzed and interpreted the data; Contributed reagents, materials, analysis tools or data; Wrote the paper.

Pengbo Chang: Performed the experiments; Analyzed and interpreted the data; Wrote the paper.

Peng Ding: Conceived and designed the experiments; Performed the experiments; Analyzed and interpreted the data.

Shuang Liu: Performed the experiments; Analyzed and interpreted the data; Wrote the paper.

Qi Rao: Performed the experiments; Analyzed and interpreted the data.

Oseweuba Valentine Okoro: Analyzed and interpreted the data; Wrote the paper.

Lingling Wang, Lihong Fan: Conceived and designed the experiments; Analyzed and interpreted the data; Contributed reagents, materials, analysis tools or data.

Amin Shavandi: Conceived and designed the experiments; Analyzed and interpreted the data; Wrote the paper.

Funding statement

This work was supported by Health Commission of Hubei Province scientific research project [WJ2019M038].

This work was supported by Wuhan Municipal Health Commission scientific research project [WX18C23].

Data availability statement

Data will be made available on request.

Declaration of interest's statement

The authors declare no conflict of interest.

Acknowledgements

We acknowledge the help from Prof. Qiuju Zhou, Dr. Zongwen Zhang, and Dr. Dongli Xu, in the Analysis & Testing Center of XYNU.

Appendix A. Supplementary data

Supplementary data to this article can be found online at https://doi.org/10.1016/j.heliyon.2023.e14349.

References

[1] X. Zhou, et al., A macaca fascicularis knee osteoarthritis model developed by modified hulth combined with joint scratches, Med. Sci. Mon. Int. Med. J. Exp. Clin. Res.: Int. Med. J. Exp. Clin. Res. 24 (2018) 3393.
[2] M.A. Szychlinska, et al., Co-expression and co-localization of cartilage glycoproteins CHI3L1 and lubricin in osteoarthritic cartilage: morphological, immunohistochemical and gene expression profiles, Int. J. Mol. Sci. 17 (3) (2016) 359.
[3] R. Bitton, The economic burden of osteoarthritis, Am. J. Manag. Care 15 (8 Suppl) (2009) S230–S235.
[4] E.N. Ringdahl, S. Pandit, Treatment of knee osteoarthritis, Am. Fam. Physician 83 (11) (2011) 1287–1292.
[5] D.O. Clegg, et al., Glucosamine, chondroitin sulfate, and the two in combination for painful knee osteoarthritis, N. Engl. J. Med. 354 (8) (2006) 795–808.
[6] E. Manheimer, et al., Meta-analysis: acupuncture for osteoarthritis of the knee, Ann. Intern. Med. 146 (12) (2007) 868–877.
[7] M. Rondanelli, et al., Clinical trials on pain lowering effect of ginger: a narrative review, Phytother Res. 34 (11) (2020) 2843–2856.
[8] D. Gregori, et al., Association of pharmacological treatments with long-term pain control in patients with knee osteoarthritis: a systematic review and meta-analysis, JAMA 320 (24) (2018) 2564–2579.
[9] N. Bellamy, et al., Intraarticular corticosteroid for treatment of osteoarthritis of the knee, Cochrane Database Syst. Rev. (2) (2006).
[10] P. Jüni, et al., Intra-articular corticosteroid for knee osteoarthritis, Cochrane Database Syst. Rev. (10) (2015).
[11] S.T. Skou, et al., A randomized, controlled trial of total knee replacement, N. Engl. J. Med. 373 (17) (2015) 1597–1606.

[12] C. Ossendorf, et al., Autologous chondrocyte implantation (ACI) for the treatment of large and complex cartilage lesions of the knee, Sports Med. Arthrosc. Rehabil. Ther. Technol. 3 (1) (2011) 1–5.
[13] S. Oussedik, K. Tsitskaris, D. Parker, Treatment of articular cartilage lesions of the knee by microfracture or autologous chondrocyte implantation: a systematic review, Arthrosc. J. Arthrosc. Relat. Surg. 31 (4) (2015) 732–744.
[14] C.T. Laurencin, L.S. Nair, The Quest toward limb regeneration: a regenerative engineering approach, Regener. Biomater. 3 (2) (2016) 123–125.
[15] L. Nie, et al., Injectable cell-laden poly (N-isopropylacrylamide)/chitosan hydrogel reinforced via graphene oxide and incorporated with dual-growth factors, Mater. Lett. 280 (2020), 128572.
[16] L. Nie, et al., Composite hydrogels with the simultaneous release of VEGF and MCP-1 for enhancing angiogenesis for bone tissue engineering applications, Appl. Sci. 8 (12) (2018) 2438.
[17] Y. Ma, et al., 3D spatiotemporal mechanical microenvironment: a hydrogel-based platform for guiding stem cell fate, Adv. Mater. 30 (49) (2018), 1705911.
[18] J.L.E. Ivirico, et al., Regenerative engineering for knee osteoarthritis treatment: biomaterials and cell-based technologies, Engineering 3 (1) (2017) 16–27.
[19] A. Fatimi, et al., Natural Hydrogel-Based Bio-Inks for 3D Bioprinting in Tissue Engineering: A Review, 2022, p. 179, 8(3).
[20] A. Shavandi, et al., 3D Bioprinting of Lignocellulosic Biomaterials, 2020, 2001472, 9(24).
[21] L. Nie, et al., Temperature-sensitive star-shaped block copolymers hydrogels for an injection application: phase transition behavior and biocompatibility, J. Mater. Sci. Mater. Med. 24 (3) (2013) 689–700.
[22] D. Chen, et al., Injectable temperature-sensitive hydrogel with VEGF loaded microspheres for vascularization and bone regeneration of femoral head necrosis, Mater. Lett. 229 (2018) 138–141.
[23] P. Zou, et al., Temperature-sensitive biodegradable mixed star-shaped block copolymers hydrogels for an injection application, Polymer 53 (6) (2012) 1245–1257.
[24] Y. Ma, et al., Bioprinting-based PDLSC-ECM screening for in vivo repair of alveolar bone defect using cell-laden, injectable and photocrosslinkable hydrogels, ACS Biomater. Sci. Eng. 3 (12) (2017) 3534–3545.
[25] C. Loebel, R.L. Mauck, J.A. Burdick, Local nascent protein deposition and remodelling guide mesenchymal stromal cell mechanosensing and fate in three-dimensional hydrogels, Nat. Mater. 18 (8) (2019) 883–891.
[26] N. Fazal, N. Latief, Bombyx mori derived scaffolds and their use in cartilage regeneration: a systematic review, Osteoarthritis Cartilage 26 (12) (2018) 1583–1594.
[27] B. Gu, et al., A sandwich-like chitosan-based antibacterial nanocomposite film with reduced graphene oxide immobilized silver nanoparticles, Carbohydr. Polym. 260 (2021), 117835.
[28] T. Yuan, et al., Injectable Ultrasonication-Induced Silk Fibroin Hydrogel For Cartilage Repair And Regeneration, 2021, pp. 1213–1224, 27(17–18).
[29] M. Mirzaei, et al., Protein-Based 3D Biofabrication of Biomaterials, 2021, p. 48, 8(4).
[30] K.-Y. Wang, et al., Injectable stress relaxation gelatin-based hydrogels with positive surface charge for adsorption of aggrecan and facile cartilage tissue regeneration, J. Nanobiotechnol. 19 (1) (2021) 214.
[31] M. Hou, et al., Biomimetic melatonin-loaded silk fibroin/GelMA scaffold strengthens cartilage repair through retrieval of mitochondrial functions, J. Mater. Sci. Technol. 146 (2023) 102–112.
[32] W. Xiao, et al., Cell-laden interpenetrating network hydrogels formed from methacrylated gelatin and silk fibroin via a combination of sonication and photocrosslinking approaches, Mater. Sci. Eng. C 99 (2019) 57–67.
[33] H. Hong, et al., Digital light processing 3D printed silk fibroin hydrogel for cartilage tissue engineering, Biomaterials 232 (2020), 119679.
[34] K. Zheng, et al., BMSCs-seeded interpenetrating network GelMA/SF composite hydrogel for articular cartilage repair, J. Funct. Biomater. 14 (1) (2023) 39.
[35] R. Zhang, et al., Mesenchymal stem cell related therapies for cartilage lesions and osteoarthritis, Am. J. Tourism Res. 11 (10) (2019) 6275.
[36] A.Q.A. Teo, et al., Equivalent 10-year outcomes after implantation of autologous bone marrow–derived mesenchymal stem cells versus autologous chondrocyte implantation for chondral defects of the knee, Am. J. Sports Med. 47 (12) (2019) 2881–2887.
[37] K. Johnson, et al., A stem cell–based approach to cartilage repair, Science 336 (6082) (2012) 717–721.
[38] J. Yang, et al., Cell-laden hydrogels for osteochondral and cartilage tissue engineering, Acta Biomater. 57 (2017) 1–25.
[39] Y. Zhu, et al., Basic science and clinical application of platelet-rich plasma for cartilage defects and osteoarthritis: a review, Osteoarthritis Cartilage 21 (11) (2013) 1627–1637.
[40] K.L. Bennell, D.J. Hunter, K.L. Paterson, Platelet-rich plasma for the management of hip and knee osteoarthritis, Curr. Rheumatol. Rep. 19 (5) (2017) 1–10.
[41] W. Kanchanatawan, et al., Short-term outcomes of platelet-rich plasma injection for treatment of osteoarthritis of the knee, Knee Surg. Sports Traumatol. Arthrosc. 24 (5) (2016) 1665–1677.
[42] K. Rahali, et al., Synthesis and characterization of nanofunctionalized gelatin methacrylate hydrogels, Int. J. Mol. Sci. 18 (12) (2017).
[43] J.W. Nichol, et al., Cell-laden microengineered gelatin methacrylate hydrogels, Biomaterials 31 (21) (2010) 5536–5544.
[44] M.G. Mehrabani, et al., Preparation of biocompatible and biodegradable silk fibroin/chitin/silver nanoparticles 3D scaffolds as a bandage for antimicrobial wound dressing, Int. J. Biol. Macromol. 114 (2018) 961–971.
[45] L. Nie, et al., Development of chitosan/gelatin hydrogels incorporation of biphasic calcium phosphate nanoparticles for bone tissue engineering, J. Biomater. Sci. Polym. Ed. 30 (17) (2019) 1636–1657.
[46] L. Nie, et al., Temperature responsive hydrogel for cells encapsulation based on graphene oxide reinforced poly (N-isopropylacrylamide)/Hydroxyethyl-Chitosan, Mater. Today Commun. (2022), 103697.
[47] L. Nie, et al., Nanostructured selenium-doped biphasic calcium phosphate with in situ incorporation of silver for antibacterial applications, Sci. Rep. 10 (1) (2020) 1–14.
[48] C. Efeoglu, Y.D. Akçay, S. Ertürk, A modified method for preparing platelet-rich plasma: an experimental study, J. Oral Maxillofac. Surg. 62 (11) (2004) 1403–1407.
[49] R. Dhurat, M. Sukesh, Principles and methods of preparation of platelet-rich plasma: a review and author's perspective, J. Cutan. Aesthetic Surg. 7 (4) (2014) 189.
[50] A. Xiang, et al., Laser photobiomodulation for cartilage defect in animal models of knee osteoarthritis: a systematic review and meta-analysis, Laser Med. Sci. 35 (4) (2020) 789–796.
[51] S. Koushesh, et al., The osteoarthritis bone score (OABS): a new histological scoring system for the characterisation of bone marrow lesions in osteoarthritis, Osteoarthritis Cartilage 30 (5) (2022) 746–755.
[52] S. Koushesh, et al., Development of a novel histological scoring system for bone marrow lesions-the osteoarthritis bone score, Osteoarthritis Cartilage 28 (2020) S124–S125.
[53] S. Mazzi, et al., Comparative thermal analysis of Eri, Mori, Muga, and Tussar silk cocoons and fibroin fibers, J. Therm. Anal. Calorimetry 116 (3) (2014) 1337–1343.
[54] Q. Wu, et al., Mercaptolated chitosan/methacrylate gelatin composite hydrogel for potential wound healing applications, Compos. Commun. 35 (2022), 101344.
[55] J. Jang, et al., Effects of alginate hydrogel cross-linking density on mechanical and biological behaviors for tissue engineering, J. Mech. Behav. Biomed. Mater. 37 (2014) 69–77.
[56] M. Sun, et al., Synthesis and properties of gelatin methacryloyl (GelMA) hydrogels and their recent applications in load-bearing tissue, Polymers 10 (11) (2018) 1290.
[57] L. Nie, et al., Injectable vaginal hydrogels as a multi-drug carrier for contraception, Appl. Sci. 9 (8) (2019) 1638.
[58] J. Huang, et al., 3D bioprinting of hydrogels for cartilage tissue engineering, Gels 7 (3) (2021) 144.
[59] S.S. Stalling, S.B. Nicoll, Fetal ACL fibroblasts exhibit enhanced cellular properties compared with adults, Clin. Orthop. Relat. Res. 466 (12) (2008) 3130–3137.

[60] A.M.T. Lubis, et al., Comparison of weekly and single dose intraarticular recombinant human growth hormone injection on cartilage degeneration in osteoarthritic model of white New Zealand rabbits, J. Experim. Orthop. 9 (1) (2022) 1–7.
[61] Y. Zhang, et al., Facile fabrication of a biocompatible composite gel with sustained release of aspirin for bone regeneration, Bioact. Mater. 11 (2022) 130–139.
[62] W. Wei, et al., Advanced hydrogels for the repair of cartilage defects and regeneration, Bioact. Mater. 6 (4) (2021) 998–1011.
[63] X. Gao, et al., Fabrication And Properties Of An Injectable Sodium Alginate/PRP Composite Hydrogel As A Potential Cell Carrier For Cartilage Repair, 2019, pp. 2076–2087, 107(9).
[64] Y.-t. Zhang, et al., Repair of osteochondral defects in a rabbit model using bilayer poly (lactide-co-glycolide) scaffolds loaded with autologous platelet-rich plasma, Med. Sci. Mon. Int. Med. J. Exp. Clin. Res.: Int. Med. J. Exp. Clin. Res. 23 (2017) 5189.